JOM, Vol. 67, No. 1, 2015
DOI: 10.1007/s11837-014-1235-1

Scalable Fabrication of Metal Oxide Functional Materials and Their Applications in High-Temperature Optical Sensing

AIDONG YAN,[1] ZSOLT L. POOLE,[1] RONGZHANG CHEN,[1] PAUL W. LEU,[2] PAUL OHODNICKI,[3] and KEVIN P. CHEN[1,4,5]

1.—Department of Electrical and Computer Engineering, University of Pittsburgh, Pittsburgh, PA 15261, USA. 2.—Department of Industrial Engineering, University of Pittsburgh, Pittsburgh, PA 15261, USA. 3.—National Energy Technology Laboratory, 626 Cochrans Mill Road, Pittsburgh, PA 15236, USA. 4.—e-mail: pec9@pitt.edu. 5.—e-mail: pchenc@gmail.com

We report a scalable manufacturing approach to produce nano-porous metal oxide films and the dopant variants using a block-copolymer template combined with a sol–gel solution processing approach. The refractive index of the film can be tailored to 1.2–2.4 by 3D nanostructuring in the sub-wavelength regime at scales of 20 nm or less. Based on this approach, this paper reports the synthesis of nanoporous palladium (Pd)-doped titanium dioxide (TiO_2) film with refractive index matching the optical fiber material, and its importance on D-shaped fiber Bragg grating for hydrogen sensing at extremely high temperature up to 700°C. The sensor is based on evanescent field interaction in hydrogen-sensitive cladding. The flat side of D-shaped fiber grating was etched to remove a residual 4 μm cladding material, and thermally stabilized for high-temperature requirements. The peak intensity change of the fiber Bragg wavelength was observed with different hydrogen concentrations from 0.25 vol.% H_2/N_2 to 5 vol.% H_2/N_2. The experimental result shows that the sensor's hydrogen response is reversible and fast. The response time of the hydrogen sensor is <8 s.

INTRODUCTION

Metal oxides are an important class of functional materials with a wide range of applications in biological and chemical sensing, optical coating, renewable energy, etc. All these applications rely on proper development and fabrication of metal oxides in various thin-film forms with desired optical or electronic properties. One of the important material parameters for metal oxide films is about their refractive indices. The functionality of these metal oxide materials depends on the tuning ranges of their refractive indices. For example, high-performance anti-reflection coatings on photovoltaic solar cells need multi-layer coating of metal oxide with refractive indices n from $\sim$1.05 to 2.2. These metal oxide optical films have been produced using conventional semiconductor processing techniques such as sputtering coating. Controls of refractive indices of optical films are typically achieved by switching different metal oxide materials and through highly specialized vacuum deposition schemes. However, these traditional manufacturing schemes are limited either by the availability of useful materials or by the lack of scalability due to its high manufacturing cost and low throughput.

In the last decade, a number of nano-engineering schemes have been developed to continuously tune the optical properties of metal oxide materials. These new manufacturing schemes provide a scalable way to explore possibilities to improve throughput and yield of existing products and to develop exciting new applications. For example, the continuous and wide range of tuning of refractive indices of optical materials can be extremely useful in transformation optics. Due to its tensorial origin,[1] most of the transformation optics designs require strong refractive index gradients for the realization of devices, which are very difficult to manufacture by conventional methods.[2]

In other applications, refractive index control enables new classes of applications that were not previously possible. The integration of these metal oxide functional materials with optical fiber for

(Published online December 9, 2014)

optical sensing is such an example. Metal oxides have been widely used for biological and chemical sensing. Most of these sensors are conductometric electronic sensors, in which conductivity of metal oxide with specific dopant and nanostructure can be selectively influenced by surface adsorption of chemical species. However, metal oxides have a typical refractive index larger than 2, which is significantly higher than that of the core of silica fiber (~1.46). Thus, it is very difficult to integrate metal oxide on fibers for optical sensing. To date, the demonstrated metal oxide integrated optical fiber sensors have been limited to the thin-film regime (on the order of 100 nm)[3,4] to avoid guided wave coupling and loss in high-index metal oxide film. But thin coatings do not take full advantage of the interacting evanescent fields and the many developments achieved for conductometric-type sensing.

In this paper, we present a solution-based low-cost and scalable manufacturing approach to produce functional metal oxides such as TiO_2, SiO_2 and their doped variants. Using block copolymer 3D sub-wavelength nano-engineering, this paper shows that the refractive indices of functional metal oxides can be engineered from n of ~1.2 to 2.4 through the control of porosity of metal oxide with pore size between 10 nm and 15 nm. In general, the modulation of the space charge region due to the presence of a chemical species is on the order of 1–10 nm.[5–7] Nanostructuring a metal oxide on this scale ensures the full modulation of the material providing enhancements in sensitivity and response time. Through precise refractive index control, Pd-doped TiO_2 nanomaterials can be integrated on fibers with long interaction length for high-sensitivity chemical sensing at extreme temperatures up to 700°C.

SCALABLE MANUFACTURING OF METAL OXIDE NANOMATERIALS

To engineer refractive index or dielectric permittivity of metal oxides using nano-engineering scheme is a relatively old idea.[8] Based on Maxwell-Garnet effective medium theory,[8] the modification of dielectric permittivity requires that the geometrical features of nanostructures are much smaller than the wavelength of the light. Recent advances in nanomaterial synthesis have provided effective techniques to structure metal oxide materials in three dimensions at the sub-wavelength (<20 nm) scales. In this paper, block copolymers templating is used to control porosity of metal oxide at 20 nm length scale to control refractive index.

Block copolymers are an interesting type of polymers widely used for nanostructure synthesis.[9] A rich group of nanostructures can be obtained by templating with block copolymers, where in most cases polymers form interconnected structures, and functional materials infiltrate voids. From the available block copolymers, Pluronic F-127, a triblock copolymer, was chosen since it has higher temperature stability and is known to form 3D interconnected structures in most cases.[10] A block-copolymer template combined with a sol–gel solution processing approach allows the synthesis of nanoporous structured thin-film of metal oxides or silica.[10] The polymer template will be removed after pre-heat treatment and the crystalline nanoporous structure will be directly developed around the template. The porosity of the film can be tuned by controlling the mole fraction of the copolymer with respect to the metal source, which will allow us to tune the effective index of the film.

In this work, metal chlorides or alkoxides were used as the precursor of the sol–gel solution in our experiment. HCl was used as a stabilizer. Pluronic F-127 was used as the structure template. First, a certain amount of HCl (37%) and ethanol were mixed together with precursor. And different amount of Pluronic F-127 was added into the solution to obtain different porosity. Then, the solution was stirring for 1 h at 60°C on the hot plate to obtain a homogeneous solution. Afterwards, the solution was cooled to room temperature and aged for 24 h. The whole process can also be performed in the presence of dopants, such as Pd. The thin films were produced by spin coating the solutions on silicon wafers in order to characterize the refractive index of nanoporous SiO_2 and TiO_2 with different porosity. Each solution was spin-coated at 2500 rpm for 30 s on silicon wafer. The freshly coated wafers were placed in an oven and preheated to 60°C, followed by a heating treatment at 130°C for 1 h. Then, the temperature slowly increased (1°C/min) to 600°C and held there for 1 h. Afterwards, the samples were cooled to room temperature at 3°C/min. Transmission electron microscopy (TEM) was used to observe the structure of synthesized thin-film, and a spectroscopic ellipsometer was used to measure the refractive index and the porosity of the film.

To develop metal oxide sensitive to hydrogen, Pd dopants were incorporated into the TiO_2. The Pd-doped TiO_2 for sensor use was synthesized using the alkoxide route of the sol–gel method. Titanium isopropoxide $\{Ti[OCH(CH_3)_2]_4\}$ was used as precursor. Palladium chloride ($PdCl_2$) was utilized as dopant. The molar ratio of Pd and Ti was 0.03. Room-temperature 0.5 g $\{Ti[OCH(CH_3)_2]_4\}$ was added into a mixture of 2.5 g ethanol and 0.25 g HCl during stirring. Pd solution was prepared by adding 0.02 g $PdCl_2$ (corresponding to 3 at.% of Ti atoms) into 1.85 g ethanol, and 0.15 g HCl was added to enhance the solubility of $PdCl_2$. The mixture was stirred 3 h to completely dissolve the $PdCl_2$. Then, the two solutions were mixed together with 0.5 g Pluronic F-127, followed by stirring for 12 h at 60°C. Then, the solution was cooled to room temperature and aged for 24 h and ready for coating.

Figure 1a presents a TEM image of refractive index controlled TiO_2. The interconnected 3D structure with features about 20 nm regime, which

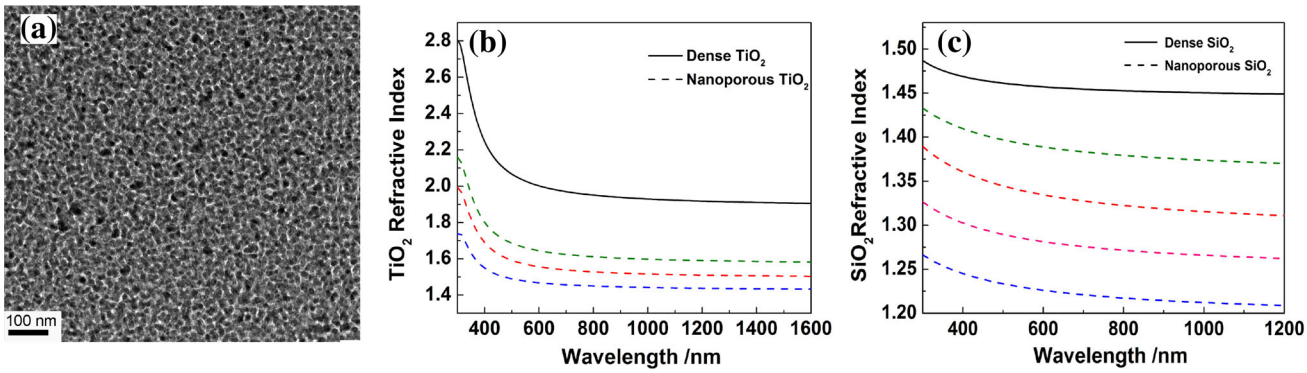

Fig. 1. (a) TEM picture of the TiO_2 film synthesized by using a block-copolymer template combined with sol–gel solution processing; refractive indices of the (b) nanoporous TiO_2, and (c) nanoporous SiO_2 film with different porosity.

are formed by the use of block copolymer Pluronic F-127, is clearly visible. The pores keep almost circular shape and are distributed uniformly. According to effective medium theory, the refractive index of a material can be lowered by introduction of non-scattering porosity.[11] This deep sub-wavelength feature formed by the block copolymers template combined with the solution processing provides a way to tailor the index of the SiO_2 and TiO_2 as we expect. Figure 1b and c summarize refractive indices of nano-porous TiO_2 and SiO_2 coated on silicon wafers with different porosity. The refractive indices were obtained by a Jobin–Yvon UVISEL spectroscopic ellipsometer. The measurement data were fit using minimization algorithms. Results presented in Fig. 1b and c show that the index of SiO_2 and TiO_2 can be modified in a large range as desired. The refractive indices of the nanoporous SiO_2 can be modified down to about n of $\sim$1.2 at 800 nm. For nano-porous TiO_2 film, the measured refractive index can be much lower than fully dense TiO_2 and the index can be modified to compatible with silica-based optical components. At 1550 nm, the index of TiO_2 with porosity 50% is about 1.43. This value is slightly lower than the D-shaped fiber intrinsic core index of 1.46, which will ensure that the light will be confined in the core of the fiber and minimize the unwanted transmission loss after coating.

INTEGRATION OF METAL OXIDE ON FIBER FOR HYDROGEN SENSING

Metal oxides have been widely used in conductometric type electronic sensors, or chemiresistors, it is well known that changes in the conductive properties are to be expected. Specific doping by certain metals, such as Al, Pd, and Pt,[12,13] are known to modify the free electron concentration and mobility of metal oxides, which can enhance their sensitivity, selectivity and response times. However, these electronic sensors cannot function in harsh environments such as extremely high temperatures (e.g., $<$500°C). In this paper, we demonstrate a fiber-optic sensing technique using metal oxide nanomaterials to perform hydrogen measurements at extremely high temperatures up to 700°C, which cannot be attained using electronic sensors.

Hydrogen has been the focus of a great amount of attention recently as a clean and environmentally friendly energy source. However, the dangers associated with the use and storage of hydrogen have always been a tremendous problem due to the wide explosive range (4–75%) and small ignition energy (0.02 mJ). Security systems monitoring of the concentration of hydrogen gas demand fast, sensitive and reliable hydrogen sensors, especially for large-scale energy generation systems where a large amount of hydrogen is stored and consumed at high temperatures. Semiconductor metal oxides such as SnO_2, TiO_2, and ZnO are widely used for hydrogen gas sensing applications due to their electrical conductivity changes after adsorption of hydrogen gas.[14–17] Despite the intrinsic properties of the material, the sensitivity to gases is also related to the structure of the sensing material, especially on the porosity and grain size.[7] Nanostructured material is believed to be more sensitive to chemicals due to the increased surface-to-volume ratios and reduced cross-sections.[5,18]Compared to other metal oxides, TiO_2 is well known for its wide band gap and structural stability at high temperatures.[5] Doping of TiO_2 has been theoretically and experimentally confirmed as a feasible way to obtain tunable semiconducting properties, which leads to the change of sensitivity.[19] Palladium is a good catalyst in oxide semiconductor hydrogen sensors. For Pd-doped TiO_2, the Pd acts as catalyst to dissociate hydrogen molecules and supply atomic hydrogen to TiO_2.

Most of the semiconductor metal oxide hydrogen sensors are electrical sensors based on resistance measurement. All-optical-fiber hydrogen sensors, due to their explosion-proof nature and immunity to electromagnetic interference, have also been developed, such as fiber Bragg grating,[20] surface plasmon resonance sensors[21] and evanescent sensors.[22] These sensors can perform effective hydrogen concentration measurements at slightly lower

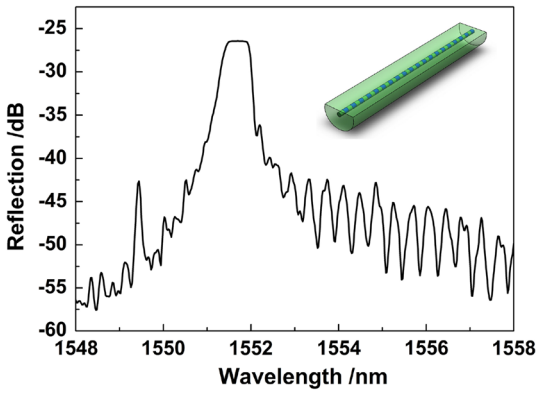

Fig. 2. Schematic of the Bragg grating inscribed on hydrogen-loaded D-shaped fiber by UV light and the reflection spectrum of the seed grating.

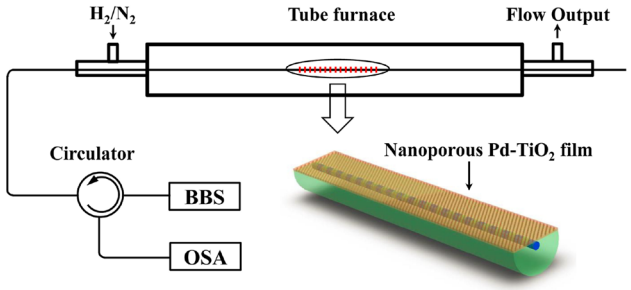

Fig. 3. Schematic diagram of Pd-TiO_2 nanoporous film coated on etched D-shaped FBG and hydrogen sensor characterization system.

temperature, usually lower than 400°C. The sensitivity of these sensors will degrade with the increase of temperature due to thermal instability. However, there are numbers of industrial applications requiring to monitor the hydrogen concentration above 600°C. To address this problem, we have developed this all-optical-fiber hydrogen sensor with Pd-doped TiO_2, which can provide rapid hydrogen concentration measurement up to 700°C. With the nanostructure in sub-wavelength regime, the refractive index of Pd-doped nanoporous TiO_2 can be tailored to match the fiber core ($n_{core} \sim 1.46$) according to effective medium theory. A rapid and ultrasensitive high-temperature hydrogen sensor was realized by using this Pd-doped nanoporous TiO_2 thin-film coated D-shaped fiber, which is an optimally designed optical fiber sensor platform.[23] High-temperature-stabilized fiber Bragg grating is induced in a D-shaped fiber for high-temperature resistance. The sensitivity of the sensor was investigated from 300°C to 700°C.

The D-shaped fiber used to prepare gratings was first soaked in pure hydrogen atmosphere at $T \sim 25$°C, $P \sim 2400$ psi for more than 2 weeks to enhance photosensitivity. Then, the strong grating with $\lambda_{bragg} = 1551.5$ nm was inscribed into the core of the D-shaped fiber by using a 248-nm KrF laser and a phase mask. The spectra and schematic of the grating are shown in Fig. 2. The grating was inscribed with strong reflection to survive high-temperature processing. In order to get a higher sensitivity, the residual 4-μm cladding material on the flat side of the D-shaped fiber was removed by placing it in a buffered HF solution (5 NH_4F:1 HF) for 21 min. After the etching process was finished, the etched grating was rinsed several times in deionized water and ethanol. Then, the grating was dried for Pd-doped TiO_2 coating.

The etched fiber with grating was immersed in the sol solution and coated through dip coating procedure at a speed of 0.2 mm/s. The coated fiber was dried in the air at room temperature overnight, and sol–gel Pd-doped TiO_2 film was formed by the hydrolysis. Then, the coated fiber was put into a tube furnace and annealed with heating to 130°C at 5 °C/min, and held there for 1 h, followed by heating to 600°C at 3°C/min and calcination for 1 h. These procedures were conducted in air atmosphere. The FBG were stabilized at the same time. After these procedures, the coated fiber was cooled to 300°C at 3°C/min, and then switched from air gas to 5 vol.% H_2/N_2 for 1 h with 40 ccm/min flow speed to reduce the PdO in the film. The schematic diagram of the D-shaped fiber Bragg grating hydrogen sensor characterization system is shown in Fig. 3. The reflection spectrum of FBG sensor was monitored by an optical spectrum analyzer. A tube furnace that could control temperature up to 800°C was used. The fiber was inserted in a quartz tube, which was placed in the tube furnace. Two rubber ferules were used to seal both ends of the tube and to apply tension to ensure that the fiber had no contact to the inner wall of the tube. The sensor can be exposed to various concentrations of hydrogen balanced with nitrogen or pure nitrogen by using two calibrated mass flow controllers. Hydrogen concentrations from 0.25 vol.% H_2/N_2 to 5 vol.% H_2/N_2 were tested in this paper.

The intensity of the Bragg resonance peak greatly depends on the index of the coating. The light can barely transmit through the coated fiber before heating treatment due to the relatively high index of the uncalcined film cladding. The index of the coated film will decrease when the Pluronic F-127 template and other organic solvent is removed by heating. In our experiment, the Bragg resonance peak disappeared after the coating and appeared again after the temperature reached 300°C. And the intensity increased via increasing temperature. Finally, the peak was stabilized at 600°C with intensity around −60 dB. Figure 4a shows the hydrogen response of the sensor in ambient cycled from pure N_2 to 5% H_2 in N_2, and then back to pure N_2 at 600°C. The intensity of the resonance peak decreased dramatically with exposure to H_2 and recovered when N_2 ambient was restored. After the system was flushed with nitrogen gas, the results were repeated with a very small amount of baseline

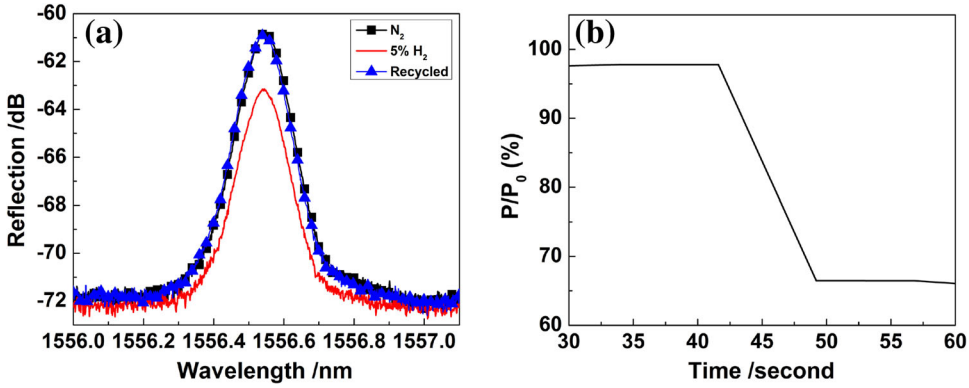

Fig. 4. (a) Spectra of the sensor cycled in 5% H_2 and N_2, (b) Response time of the hydrogen sensor.

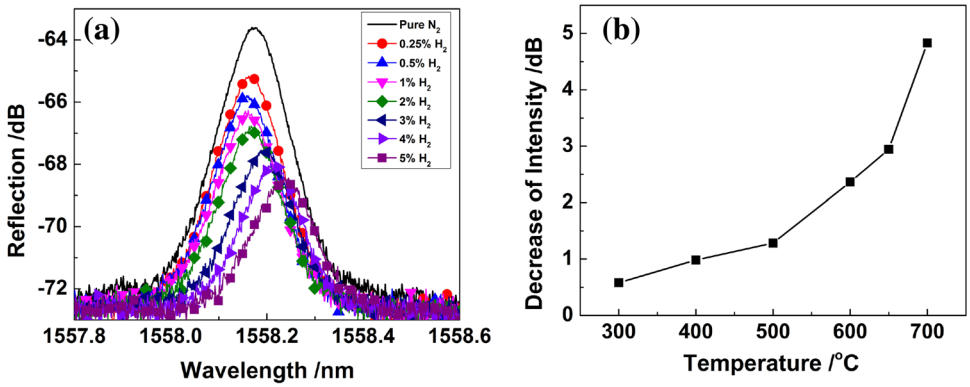

Fig. 5. (a) Spectrum of the coated D-shaped FBG exposed to 0.25%, 0.5%, 1%, 2%, 3%, 4%, 5% H_2 and pure N_2 respectively, (b) peak intensity as a function of temperature for 5% H_2.

drift. This indicates that the hydrogen sensor based on nano-porous Pd-TiO_2 coated etched D-shaped FBG is reliable at high temperature. Response time is an important sensitivity indicator of a sensor, which is defined as the time required for the sensor to reach its average lowest peak intensity. In order to measure the response time of the Pd-doped nano-porous TiO_2, the intensity of the transmission was directly measured. The response time of the sensor upon exposure to hydrogen is 7–8 s as Fig. 4b shows. The restore time of the sensor is about several minutes in pure N_2 flush. The restore time is believed to decrease dramatically if a small amount of O_2 is added into the N_2.

Figure 5a presents the reflection spectra of the FBG exposed to H_2 with concentration range from 0.25% to 5% at the highest testing temperature of 700°C. The reduction of 6 dB of FBG peak magnitude can be observed for the change of hydrogen concentration from 0% to 5%. The intensity of the peak has been decreased more compared with that at 600°C, which indicates stronger optical absorption. The reduction of FBG peak is also accompanied by a shift of the FBG peak, which is the indication of refractive index change of FBG. An 80-pm FBG wavelength shift is noted in Fig. 5a. Given that up to 2% of guided light is propagated in the Pd-doped TiO_2 coating, up to 4×10^{-3} of refractive index change could be due to the redox reaction of Pd-doped TiO_2 film.[8] However, the FBG peak shifts could also be due to temperature variation. The thermal-optic coefficient of FBG in silica fiber is ~13 pm/°C. The FBG wavelength shifts shown in Fig. 5a could be attributed to up to 7°C temperature fluctuation at the elevated temperature of 700°C. Figure 5b shows the decrease of the peak intensity upon switching ambient from N_2 to 5% H_2 as a function of temperature. The improvement of the sensor performance at high temperature is considered to be beneficial for more effective catalytic dissociation of H_2 in Pd-doped TiO_2 at higher temperatures. However, our experiments also show that the performance will degrade when the temperature goes higher than 780°C, due to thermal instability of the porosity structure at this temperature. Because the porosity structure begins to collapse when the temperature is higher than 780°C, this will decrease the surface to volume ratio and increase the refractive index of the film, resulting in large optic loss.

CONCLUSION

This paper presents a solution-based scalable nanofabrication scheme to manufacture metal

oxides and their doping variants with controlled index of refraction. Through block copolymer templating, nanoporous Pd-doped TiO_2 3D nanostructure with pore size from 5 nm to 20 nm was synthesized. Through this approach, the indices of refraction of SiO_2 and TiO_2 can be controlled over a wide range from 1.2 to 2.4. In this paper, this new material synthesis technique has been successfully applied for new optical sensor developments. Using a solution-based coating technique, Pd-doped TiO_2 functional coatings were successfully integrated with high-temperature stable fiber Bragg grating in D-shaped fibers for evanescent wave sensing for hydrogen at elevated temperatures up to 700°C. Using the same nano-synthesis scheme, it is also possible to manufacturing other metal oxides with the desired index such as SnO_2 and ZnO. Further, it is also possible to combine the solution-based processing scheme, as demonstrated in this work, with other manufacturing schemes such as dip-pen nanolithography, dip coating, or ultrasonic spraying coating to produce metal oxide coatings over large areas for scalable device fabrication at low cost.

ACKNOWLEDGEMENTS

This work was supported by the National Science Foundation (CMMI-1300273, CMMI-1348591) and the Department of Energy (DE-FE0003859). This report was prepared as an account of work sponsored by an agency of the United States Government. Neither the United States Government nor any agency thereof, nor any of their employees, makes any warranty, express or implied, or assumes any legal liability or responsibility for the accuracy, completeness, or usefulness of any information, apparatus, product, or process disclosed, or represents that its use would not infringe privately owned rights. Reference herein to any specific commercial product, process, or service by trade name, trademark, manufacturer, or otherwise does not necessarily constitute or imply its endorsement, recommendation, or favoring by the United States Government or any agency thereof. The views and opinions of authors expressed herein do not necessarily state or reflect those of the United States Government or any agency thereof.

REFERENCES

1. J.B. Pendry, D. Schurig, and D.R. Smith, *Science* 312, 1780 (2006).
2. Q. Wu, J.P. Turpin, and D.H. Werner, *Light Sci. Appl.* 1, e38 (2012).
3. N. Yamazoe, *Sens. Actuators B* 108, 2 (2005).
4. Z. Gu, Y. Xu, and K. Gao, *Opt. Lett.* 31, 2405 (2006).
5. I.D. Kim, A. Rothschild, B.H. Lee, D.Y. Kim, S.M. Jo, and H.L. Tuller, *Nano Lett.* 6, 2009 (2006).
6. N. Yamazoe, *Sens. Actuators B* 5, 7 (1991).
7. A. Rothschild and Y. Komem, *J. Appl. Phys.* 95, 6374 (2004).
8. Z. Poole, P. Ohodnicki, R. Chen, Y. Lin, and K. Chen, *Opt. Express* 22, 2665 (2014).
9. M.C. Orilall and U. Wiesner, *Chem. Soc. Rev.* 40, 520 (2011).
10. S. Shao, M. Dimitrov, N. Guana, and R. Kohn, *Nanoscale* 2, 2054 (2010).
11. B.E. Yoldas and D.P. Partlow, *Thin Solid Films* 129, 1 (1985).
12. M. Zhang, Z. Yuan, J. Song, and C. Zheng, *Sens. Actuators B* 148, 87 (2010).
13. J. Moon, J.A. Park, S.J. Lee, T. Zyung, and I.D. Kim, *Sens. Actuators B* 149, 301 (2010).
14. A. Kolmakov and M. Moskovits, *Annu. Rev. Mater. Res.* 34, 151 (2004).
15. B. Wang, L.F. Zhu, Y.H. Yang, N.S. Xu, and G.W. Yang, *J. Phys. Chem. C* 112, 6643 (2008).
16. H.T. Wang, B.S. Kang, F. Ren, L.C. Tien, P.W. Sadik, D.P. Norton, S.J. Pearton, and J. Lin, *Appl. Phys. Lett.* 86, 243503 (2005).
17. H.F. Lu, F. Li, G. Liu, Z.G. Chen, D.W. Wang, H.T. Fang, G.Q. Lu, Z.H. Jiang, and H.M. Cheng, *Nanotechnology* 19, 405504 (2008).
18. A.S. Zuruzi, A. Kolmakov, N.C. MacDonald, and M. Moskovits, *Appl. Phys. Lett.* 88, 102904 (2006).
19. H. Liu, D. Ding, C. Ning, and Z. Li, *Nanotechnology* 23, 015502 (2012).
20. M. Buric, K.P. Chen, M. Bhattarai, P.R. Swinehart, and M. Maklad, *IEEE Photonics Technol. Lett.* 19, 255 (2007).
21. X. Bevenot, A. Trouillet, C. Veillas, H. Gagnaire, and M. Clement, *Meas. Sci. Technol.* 13, 118 (2002).
22. J. Villatoro, D.L. Moreno, and D.M. Hernández, *Sens. Actuators B* 110, 23 (2005).
23. F.A. Muhammad and G. Stewart, *Electron. Lett.* 28, 1205 (1992).